JOURNAL OF QUATERNARY SCIENCE (2005) **20**(1) 21–32

Published online in Wiley InterScience (www.interscience.wiley.com). DOI: 10.1002/jqs.892

Holocene sedimentation in the Skagerrak interpreted from chirp sonar and core data

RICHARD GYLLENCREUTZ,* MARTIN JAKOBSSON and JAN BACKMAN
Department of Geology and Geochemistry, Stockholm University, Stockholm, Sweden

Gyllencreutz, R., Jakobsson, M. and Backman, J. 2005. Holocene sedimentation in the Skagerrak interpreted from chirp sonar and core data. *J. Quaternary Sci.*, **Vol. 20** pp. 21–32. ISSN 0267-8179.

Received 23 January 2004; Revised 23 July 2004; Accepted 16 August 2004

ABSTRACT: High-resolution chirp sonar profiling in the northeastern Skagerrak shows acoustically stratified sediments draping a rough-surfaced substratum. A 32 metre long sediment core retrieved from the survey area encompasses the entire Holocene and latest Pleistocene. The uppermost seismo-acoustic units in the chirp profiles represent Holocene marine sediments. The lowermost unit is interpreted as ice-proximal glacial-marine sediments rapidly deposited during the last deglaciation. The end of ice-proximal sedimentation is marked by a strong reflector, interpreted to have been formed during latest Pleistocene time as a consequence of rapid ice retreat and drastically lowered sedimentation rate. The subsequent distal glacial-marine sediments were deposited with initially high sedimentation rates caused by an isostatic rebound-associated sea-level fall. Based on correlation between the core and the chirp sonar profiles using measured sediment physical properties and AMS ^{14}C dating, we propose a revised position for the Pleistocene/Holocene boundary in the seismo-acoustic stratigraphy of the investigated area. Copyright © 2005 John Wiley & Sons, Ltd.

KEYWORDS: Holocene; Skagerrak; seismic; sediments; deglaciation.

Introduction

The Skagerrak is the deepest part of the otherwise relatively shallow North Sea (Figs 1 and 2). The North Atlantic Current mainly drives the circulation and subsequent sedimentation in the Skagerrak, with important contributions from Baltic Sea outflow and from the Jutland Current (Fig. 3) (Longva and Thorsnes, 1997). In the deep northeastern Skagerrak, mixed currents form an anticlockwise gyre reducing the current speed, which allows fine-grained sediment to accumulate at very high rates (van Weering, 1982a; Rodhe and Holt, 1996; Bøe *et al.*, 1996). For this reason, the Skagerrak is the major sink for fine-grained sediment in the North Sea. Acquired seismic reflection data shows the presence of a thick, apparently undisturbed, sediment sequence in the northeastern Skagerrak (Stabell *et al.*, 1985; van Weering *et al.*, 1993; Bøe *et al.*, 1996; Rise *et al.*, 1996; Longva and Thorsnes, 1997; Novak and Stoker, 2001). Holocene sedimentation in the Skagerrak has been comprehensively reviewed by van Weering *et al.* (1993).

The promising high-resolution sedimentary archives prompted the International Marine Past Global Changes Study (IMAGES) programme to select the coring site MD99-2286 in this area (Figs 1 and 2), where a 32 m long core was retrieved in 1999. The main objective was to study the Holocene circulation changes in the Skagerrak, in order to obtain important information about the mode and amplitude of oceanographic and climatic variability.

This paper provides a detailed view of the Holocene and latest Pleistocene stratigraphy in the northeastern Skagerrak based on high-resolution chirp sonar data acquired with R/V *Skagerrak* during the site survey for IMAGES site MD99-2286 and on studies of the 32 m long core. An age model based on 27 radiocarbon dates was established for MD99-2286 and the calibrated ages show that the core spans 12 000 years, thus encompassing the entire Holocene and the latest Pleistocene. All data was brought into a dynamic 3-D environment for the construction of a stratigraphic model and subsequent interpretation. In this paper, we will use the informal working definition of 11 500 cal. yr BP (10 000 ^{14}C years) for the base of the Holocene at the end of the Younger Dryas cold period, as assigned by the International Commission on Stratigraphy (ICS website, 2004).

Oceanographic and sedimentary setting

The Skagerrak is bordered by the coasts of Denmark, Sweden and Norway and consists of a glacially eroded sedimentary basin that forms the southeastern end of the Norwegian Trench (Flodén, 1973; Holtedahl, 1986; Sejrup *et al.*, 1995, 2000, 2003) (Fig. 1). Water depths in the Skagerrak basin exceed 700 m (Fig. 1), making it the deepest part of the otherwise shallow North Sea.

* Correspondence to: Richard Gyllencreutz, Department of Geology and Geochemistry, Stockholm University, SE-10691 Stockholm, Sweden.
E-mail: richard.gyllencreutz@geo.su.se

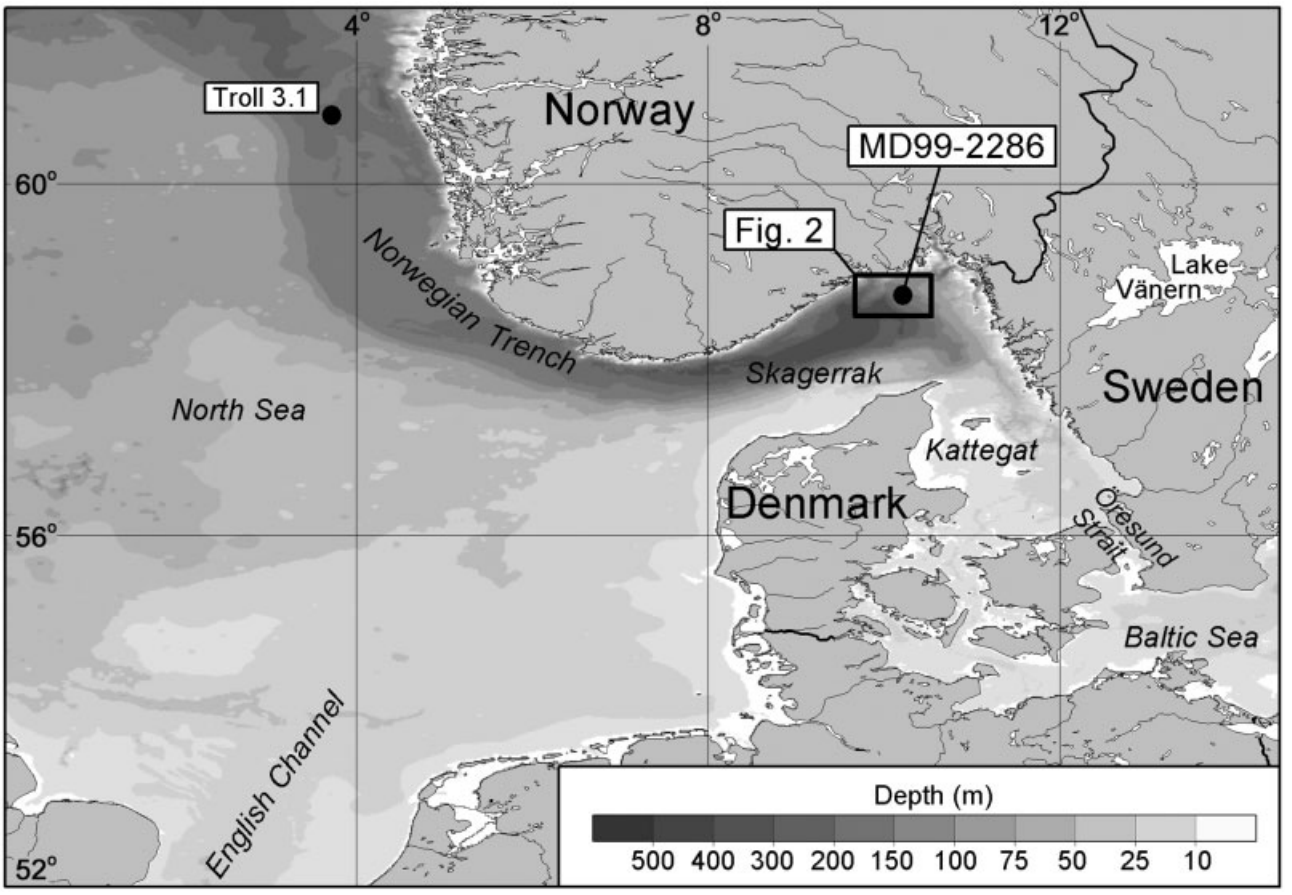

Figure 1 Bathymetry of the North Sea and adjacent areas based on the General Bathymetric Chart of the Oceans (GEBCO) Digital Atlas (GDA) (IOC, 2003). Locations of core MD99-2286, core Troll 3.1 and Fig. 2 are indicated

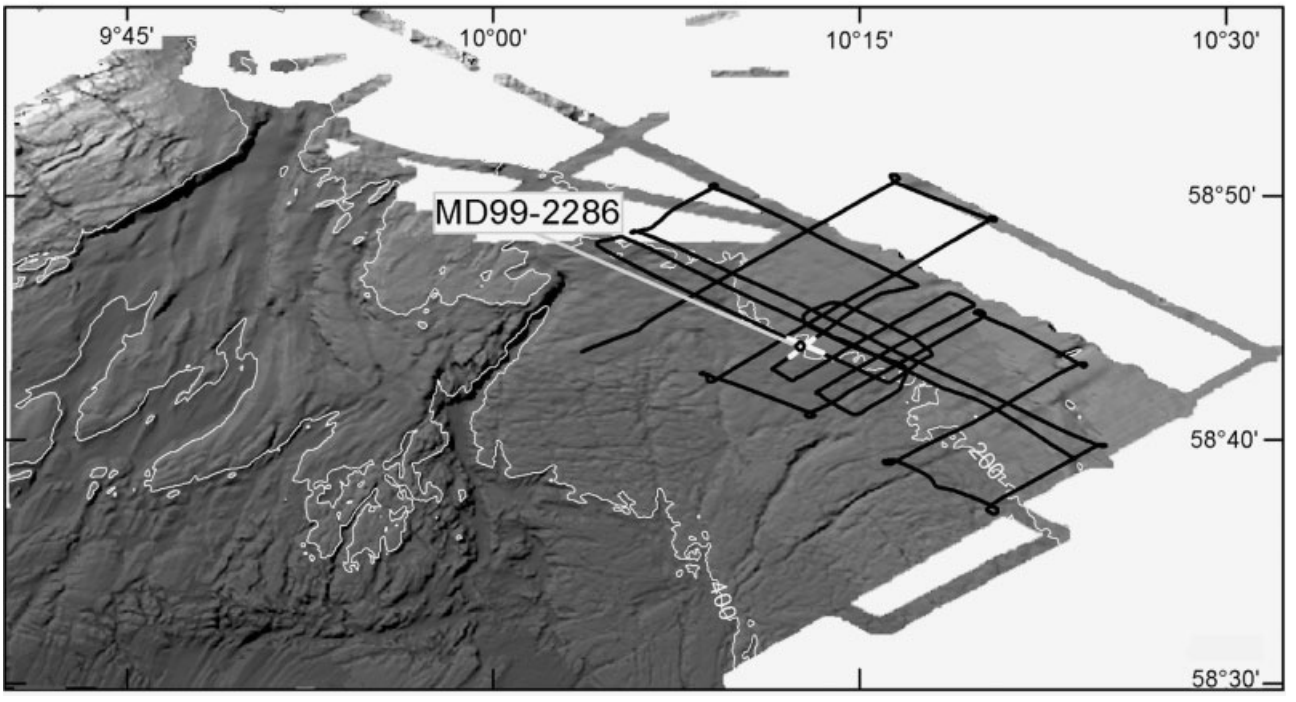

Figure 2 Chirp sonar track chart (black lines) and bathymetry of the survey area. White crossing lines indicate location of profiles at the coring target for core MD99-2286 (see Fig. 6b). Multibeam bathymetry data from the Norwegian Hydrographic Service (Ottesen *et al.*, 1997)

The following summary of present large-scale circulation in the Skagerrak is based on Svansson (1975), Rodhe (1987, 1998) and Otto *et al.* (1990). The North Atlantic Current mainly governs the circulation and subsequent sedimentation in the Skagerrak through water entering the North Sea between Scotland and Norway, along with minor inflow through the English Channel. The most important feature of the Skagerrak circulation is the Jutland Current, which is formed of mixed

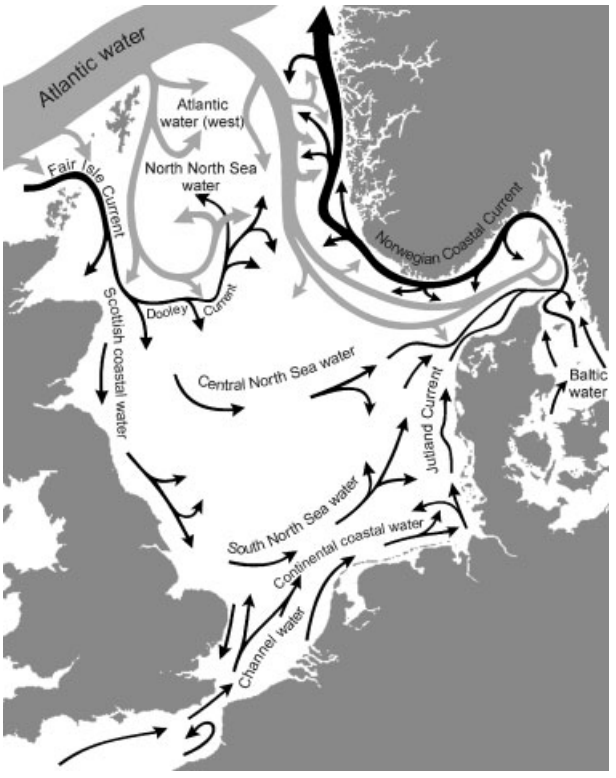

Figure 3 General circulation pattern in the North Sea and Skagerrak. The relative magnitude of volume transport is indicated by the width of the arrows. Grey arrows indicate water entering the Skagerrak more or less directly from the Atlantic and black arrows indicate indirect transport via the North Sea or from the Baltic Sea (redrawn from Longva and Thorsnes, 1997, fig. 4.3)

watermasses from the English Channel and the southern North Sea and runs northward along the Danish west coast (Fig. 3). The Jutland Current further mixes with Central North Sea water as it continues to the northeast entering the Skagerrak. Furthermore, the watermass is subsequently mixed with relatively fresh and cold Baltic Sea water, before it makes a cyclonic turn in the northeastern Skagerrak. The water then continues westward and exits the Skagerrak in the southwest as the Norwegian Coastal Current (Fig. 3). In the course of the cyclonic turn in the Skagerrak, the water depth increases and the current speed is greatly reduced, causing fine-grained sediment to be deposited in the northeastern and central parts of the Skagerrak (Rodhe and Holt, 1996) at a relatively high rate, up to 1 cm yr^{-1} (van Weering, 1982a; Bøe *et al.*, 1996). During periods with strong influence of Atlantic water from the northern passage, the Jutland Current can be blocked for a limited period, and subsequently flushed into the Skagerrak in 2–3 weeks when the Atlantic inflow diminishes again (Aure *et al.*, 1990).

Most of the suspended sediment entering the Skagerrak is derived from the large amounts of inflowing Atlantic water with low sediment concentration (Longva and Thorsnes, 1997), with important contributions from the Jutland Current carrying a high sediment load of erosion products from the Jutland coasts (Eisma and Kalf, 1987).

The present water depth is 225 m at the coring site, and the accumulated sediment thickness as interpreted from chirp sonar profiles is about 55 m. This corresponds to ca. 75 milliseconds (ms) two-way travel time (TWT), using a sediment sound velocity of 1500 m s^{-1}; this value is always used for converting TWT to metres in this study, and all values below given in milliseconds refer to TWT. Using a sea level of 160–180 m above present sea level just after the last deglaciation (Hafsten, 1983; Lambeck *et al.*, 1998) and correcting for the sediment accumulation, the palaeo-water depth at the coring site at the time of the deglaciation was about 400–450 m.

The Skagerrak was a fjord-like basin during the deglaciation (Stabell and Thiede, 1986) until a seaway developed across middle Sweden after the final drainage of the Baltic Ice Lake at ca. 11 560 calendar years BP (Björck, 1995; Andrén *et al.*, 2002; Björck *et al.*, 2002). The former land region west of Jutland was flooded at about the same time, resulting in a major change of the geographic position of the southern coastlines (Stabell and Thiede, 1985, 1986). Another major change in the hydrographic conditions in the Skagerrak was the opening of the English Channel at about 7500–7600 ^{14}C years BP (Jelgersma, 1979; Nordberg, 1991; Conradsen and Heier-Nielsen, 1995; Lambeck, 1995; Knudsen and Seidenkrantz, 1998), equivalent to ca. 8500 cal. yr BP using the MARINE98 calibration curve. The major components of the modern circulation system were established in conjunction with a hydrographic shift at 5500 ^{14}C years BP (Conradsen, 1995; Conradsen and Heier-Nielsen, 1995; Jiang *et al.*, 1997), equivalent to ca. 6400 cal. yr BP. This shift is interpreted as an increase in the Jutland Current and stronger inflow of saline North Sea water to the Skagerrak and the Kattegat, synchronous with the final drowning of the Jutland Bank (Leth, 1996).

Previous seismic surveys and coring in the study area

In previous seismic reflection studies of the Skagerrak and the Norwegian Trench, an uppermost acoustic unit has been defined and described as acoustically transparent, and proposed to be of Holocene age (van Weering *et al.*, 1973; van Weering, 1975; van Weering, 1982b; Fält, 1982; Holtedahl, 1986; Salge and Wong, 1988; von Haugwitz and Wong, 1993; Andersen *et al.*, 1995b; Rise *et al.*, 1996). In these investigations various systems such as Airgun, Sleeve gun, Sparker, Boomer or GeoPulse were used as seismic sources. In a seismic survey of outer Oslo Fjord sediments, an uppermost acoustically transparent unit, of supposedly Holocene or late glacial age, was described by Solheim and Grønlie (1983). Novak and Stoker (2001) suggested that a parallel-stratified acoustic unit in the southern Skagerrak comprised the Holocene, interpreted from deep-towed Boomer data.

Previous coring in the region comprises at least 15 cores longer than 2 m, including the more than 200-m long Skagen 3 core, drilled onshore in northernmost Denmark, and the 38-m long Troll 3.1 core from the Norwegian Channel (Andersen *et al.*, 1995b). In addition, the surface sediments and recent sedimentation rates in the Norwegian part of the Skagerrak have been investigated in the study of 268 short cores (<50 cm), collected within the 'Skagerrak project' (Bøe *et al.*, 1996; Ottesen *et al.*, 1997; Longva and Thorsnes, 1997). With the exception of the Skagen 3 core, MD99-2286 is the longest core retrieved from the Skagerrak that spans the entire Holocene. None of the previous cores from the Skagerrak have been correlated to seismic profiles to permit dating of acoustic reflectors.

Methods

Coring

A 32.4 m long CALYPSO core, MD99-2286, was retrieved in 1999 from 225 water depth by R/V *Marion Dufresne* at

58°43.77′ N, 10°12.31′ E (Fig. 1), using a 40 m long core barrel. The CALYPSO corer is a giant version of the conventional piston core, capable of retrieving up to ~60 m long cores. A dual ('breakaway') piston design is incorporated in the coring system to minimise coring disturbance during recovery (pull-out) from the seafloor (Rack *et al.*, 2000). In addition, a 2.4 m long gravity core, Sk000209-2, was retrieved in 2000 from 225 m water depth by R/V *Skagerrak* at 58°43.84′ N, 10°11.78′ E (622 m from core MD99-2286) in order to ensure full recovery of the surface sediments.

Core description

Following the splitting of core MD99-2286, the sediment was visually described with respect to macro-sedimentology, colour (using the Munsell soil colour chart) and macrofossils onboard the ship. The microfossil content was described in 18 smear slides evenly distributed along the 32 m long core.

Physical properties

Whole-core logging of Gamma Ray Attenuation (GRA) density (Fig. 4a) was performed onboard R/V *Marion Dufresne* using a GeoTek Multi Sensor Core Logger (MSCL). High-resolution point measurements of p-wave velocity were carried out on split core halves at the Department of Geology and Geochemistry, Stockholm University, also using a GeoTek MSCL (Fig. 4b). Prior to the physical property measurements, the core was stored in the core-logging laboratory until the sediment attained a stable temperature. P-wave measurements were also carried out on three discrete samples in constant-volume containers from the top, middle and bottom of the core, on a GeoTek MSCL at the University of Rhode Island.

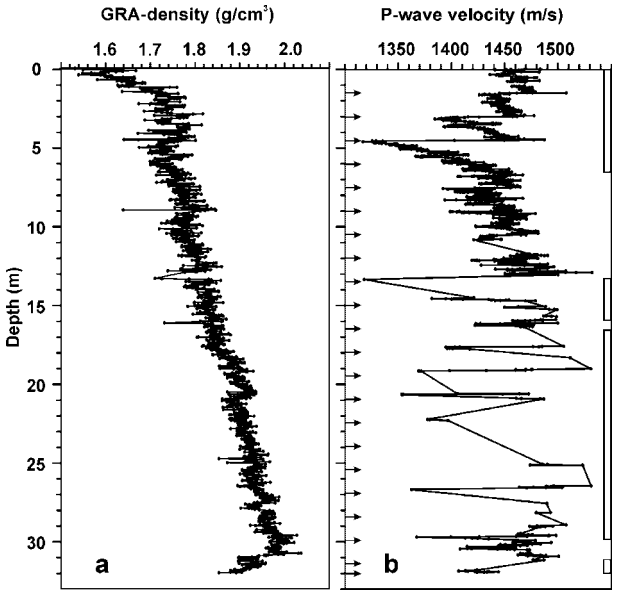

Figure 4 MST-measured physical properties plotted against depth (m) in core MD99-2286. (a) Boyce-corrected (Boyce, 1976) GRA-density measured with 2-cm resolution. (b) P-wave velocity, measured with 0.5-cm resolution. The p-wave data was calibrated to on-site conditions using a temperature of 7 °C (Svansson, 1975), a salinity of 35‰ (Svansson, 1975; Rodhe, 1987) and a water depth of 225 m. Arrows indicate core section breaks. The outlined bars in right side of (b) indicate depth intervals where artefacts occur and where the signal was lost due to bad transducer coupling

Dating

The chronostratigraphic control of core MD99-2286 relies on 27 AMS ^{14}C dates, performed by the Institute of Particle Physics, ETH, Zurich, Switzerland, using the method described by Hajdas *et al.* (1997). The dated samples consist of either mollusc shells of known species or mixed benthic foraminifera. The radiocarbon dates were calibrated using the CALIB (rev. 4.4) software (Stuiver and Reimer, 1993). The samples were assumed to consist of 100% marine carbon, and the calibration data set MARINE98 (Stuiver *et al.*, 1998) was used. In order to facilitate comparison with other studies, a standard reservoir correction of 400 years was used for all samples, although we recognise that the reservoir age may have been greater during part or all of the deglaciation (Bard *et al.*, 1990; Bondevik *et al.*, 1999). The results of the calibrated AMS ^{14}C dates are presented using the probability method (Telford *et al.*, 2004) (Table 1 and Fig. 5).

Chirp sonar profiling

High-resolution seismo-acoustic data was acquired from R/V *Skagerrak* with an EdgeTech X-Star chirp sonar system using the SB-512 tow-fish. The reflected acoustic signal was digitally recorded after real time processing through a correlation filter (Schock *et al.*, 1989). Surveying was performed with a 40 ms long 1.5–7.5 kHz chirp pulse, resulting in a sediment penetration of between 40 and 90 ms in water depths ranging between 100 and 300 m, yielding a vertical resolution of ca. 12 cm. The total length of chirp profiles collected in this study is 217 km (Fig. 2). The positioning system consisted of a differential GPS. Soundings from the ship's hull-mounted Skipper GDS 101 echo sounding system were used to adjust variations in the chirp sonar tow-fish depth.

Dynamic 3-D visualisation

All data in this study (i.e. chirp sonar, bathymetry, and core data) together with multi-beam bathymetry from the Geological Survey of Norway was brought into Interactive Visualization System's (IVS) dynamic 3-D visualisation software Fledermaus (Mayer *et al.*, 2000). Grey-scale raster images were prepared from the processed chirp sonar data using an average sound speed of 1500 m s^{-1} and displayed geo-referenced as 'hanging curtains'. The geological interpretation of the high-resolution chirp sonar data was undertaken in this 3-D environment, which greatly facilitated a consistent interpretation due to the simultaneous display of crossing lines. The 3-D visualisation also provided a quality check of the chirp sonar depth measurements using the detailed multi-beam bathymetry (Figs 2 and 6).

Results

Lithology

The visual sedimentological description reveals that core MD99-2286 consists of nearly homogeneous silty clay, which slightly coarsens upwards. The sediment colour showed variations ranging from dark olive grey (Munsell colour 5Y3/2) to dark greenish grey (Munsell colour 5Y4/1). Slight colour

Table 1 AMS ^{14}C dating of core MD99-2286 (MD) and core Sk000209-2 (Sk). Laboratory reference codes in parentheses denote samples omitted from the age model due to presumed sediment reworking. The results from core Sk000209-2 are from Senneset (2002). Laboratory reference codes in parentheses denote samples omitted from the age model

Laboratory reference	Core	Corr. depth[a] (cm)	Nominal depth (cm)	$\delta^{13}C$ vs. PDB ‰	+/− 1σ	^{14}C age (Libby h.l.) (^{14}C yr BP)	+/− 1σ	Age range (cal. yr BP) probability method Max. (1σ)	Median	Min. (1σ)	Dated species	Weight (mg)	Type[b]
(ETH-24 953)	MD	115.5	115.5	−3.8	1.2	785	50	480	424	378	Scaphander *sp.*	27.78	g,w
(ETH-25 546)	MD	185.5	185.5	2.0	1.2	800	55	494	436	393	*Yoldiella lucida*	8.85	m,w
ETH-24 001	MD	268	268	1.7	1.2	535	50	252	166	113	*Ennucula tenuis*	26.1	m,w
ETH-24 397	MD	319.5	319.5	1.8	1.2	730	45	417	372	320	*Thyasira equalis*	49.67	m,b
(ETH-26 937)	MD	319.5	319.5	0.5	1.2	1095	55	701	652	613	Foraminifera (mixed fauna)	11.86	f
ETH-25 547	MD	370.5	370.5	0.7	1.2	900	60	548	513	467	*Nucula tumidula*	9.55	m,b
(ETH-26 388)	MD	410.5	410.5	0.1	1.2	1270	50	877	814	761	Foraminifera (mixed fauna)	13.07	f
ETH-26 938	MD	481.5	481.5	2.7	1.2	1225	55	824	768	699	Foraminifera (mixed fauna)	16.77	f
(ETH-26 939)	MD	561	561	−0.1	1.2	1510	50	1115	1057	992	Foraminifera (mixed fauna)	18.57	f
ETH-26 940	MD	640.5	640.5	0.8	1.2	1530	50	1146	1080	1024	Foraminifera (mixed fauna)	16.23	f
(ETH-25 955)	MD	700.5	700.5	2.3	1.2	1915	55	1518	1458	1398	Foraminifera (mixed fauna)	16.42	f
ETH-25 956	MD	801	801	−0.2	1.2	1915	55	1518	1458	1398	Foraminifera (mixed fauna)	18.04	f
(ETH-26 389)	MD	901	901	0.5	1.2	2155	50	1808	1744	1690	Foraminifera (mixed fauna)	19.29	f
ETH-26 390	MD	1001	1001	−0.5	1.2	2175	50	1819	1766	1705	Foraminifera (mixed fauna)	15.51	f
ETH-26 941	MD	1070.5	1070.5	3.0	1.2	2440	55	2138	2076	1997	Foraminifera (mixed fauna)	11.62	f
ETH-26 418	MD	1200.5	1200.5	1.4	1.2	2765	60	2572	2493	2360	Foraminifera (mixed fauna)	12.56	f
ETH-27 241	MD	1360.5	1400.5	0.0	1.2	2975	55	2789	2752	2704	Foraminifera (mixed fauna)	14.87	f
(ETH-26 419)	MD	1460.5	1500.5	1.3	1.2	3390	60	3334	3256	3192	Foraminifera (mixed fauna)	14.05	f
(ETH-27 242)	MD	1660.5	1700.5	−1.7	1.2	3895	60	3952	3861	3775	Foraminifera (mixed fauna)	18.1	f
ETH-26 137	MD	1826	1866	1.0	1.2	4120	60	4252	4173	4081	*Polinices montagui*	16.73	g,w
ETH-24 003	MD	2377	2417	1.3	1.2	6255	65	6773	6698	6628	*Portlandia intermedia*	42.6	m,b
ETH-25 548	MD	2676.5	2716.5	3.4	1.2	7955	70	8478	8410	8335	*Pseudamusium septemradiatum*	62.37	m,b
(ETH-25 549)	MD	2681.5	2721.5	2.9	1.2	7710	60	8262	8163	8099	*Pseudamusium septemradiatum*	100.02	m,b
ETH-25 550	MD	3100.5	3140.5	−0.6	1.2	9620	70	10 585	10 332	10 145	*Pseudamusium septemradiatum*	44.68	m,b
ETH-24004	MD	3119	3159	1.1	1.2	9955	85	11 080	10 734	10 373	*Bathyarca glacialis*	25.5	m,b
ETH-25 551	MD	3129.5	3169.5	−2.0	1.2	9910	70	11 003	10 696	10 354	*Cryptonautica affinis*	25.77	g,b
ETH-24 005	MD	3198	3238	1.4	1.2	10 715	80	12 306	11 954	11 678	*Portlandia intermedia*	134.5	m,b
KIA13 258	Sk		100–101	—	—	605	30	279	266	256	Not identified	1.0[c]	m-,b
KIA13 259	Sk		160–161	—	—	915	35	536	516	500	Not identified	0.4[c]	m-,b

[a] Correction for artificial void in core at 1315–1355 cm; nominal depths below 1355 cm are reduced by 40 cm.
[b] Type abbreviations: g = gastropod, m = mollusc, f = benthic foraminifera, w = whole, b = broken.
[c] The weight of core Sk000209-2 samples is given in pure carbon (mg C).

mottling, possibly indicating bioturbation, was observed throughout the core. Sulphide streaks and small cracks, indicating reducing conditions and the presence of gas, were observed in the intervals 0–15 m and 24–29 m. During the core description, a void in the core at 13.15–13.55 m depth was noted. The sediment on both sides of the void was firm and apparently undisturbed, and the facing edges of the void perfectly matched each other. As no sediment appears to be missing, this void is regarded as an artificial effect from the coring, and therefore the length of the void (40 cm) was subtracted from the nominal core depth from 13.55 m downwards.

Sediment physical properties

The GRA density record of core MD99-2286 shows a rapid down-core increase from ca. 1.6 to ca. 1.7 g cm^{-3} in the top 2 m of the core (Fig. 4a). From 2 m, the density increases linearly to almost 2.0 g cm^{-3} at 31 m core depth, attributed to post-depositional compaction of the sediment. The lowermost metre of the core is characterised by a down-core decrease in density reaching ca. 1.9 g cm^{-3} in the bottom of the core.

The p-wave record of core MD99-2286 shows values ranging from 1400 to 1550 m s^{-1} (Fig. 4b). The discrete sample p-wave measurements yielded velocities of 1540.4 m s^{-1} at 2.94–2.99 m, 1573.5 m s^{-1} at 14.54–14.59 m and 1491.9 m s^{-1} at 30.95–31.00 m depth. However, artefacts related to core section breaks in the top of the core and lack of useful p-wave velocity data below 13 m (Fig. 4b), possibly caused by small amounts of gas trapped between the core liner and the sediment, preclude the use of p-wave velocity for a synthetic seismogram that could be used for core correlation to the chirp sonar records. Therefore, the p-wave data are only used as an approximation of the seismic velocity.

Chronostratigraphy

The calibrated ages show that core MD99-2286 spans 0 to 11 680–12 300 years (one-sigma age range), and thus covers the entire Holocene and the latest Pleistocene (Fig. 5). The inferred sedimentation rate gradually increases with time, from 0.06 cm yr^{-1} at 12 000 yr BP to about 1 cm yr^{-1} in the uppermost sediments. The latter is consistent with the measured modern sediment accumulation rates of >0.6 cm yr^{-1} around the coring site (Bøe *et al.*, 1996).

Some of the AMS ^{14}C dates in the core are problematic, especially in the top 10 m, as some ages are older than or identical

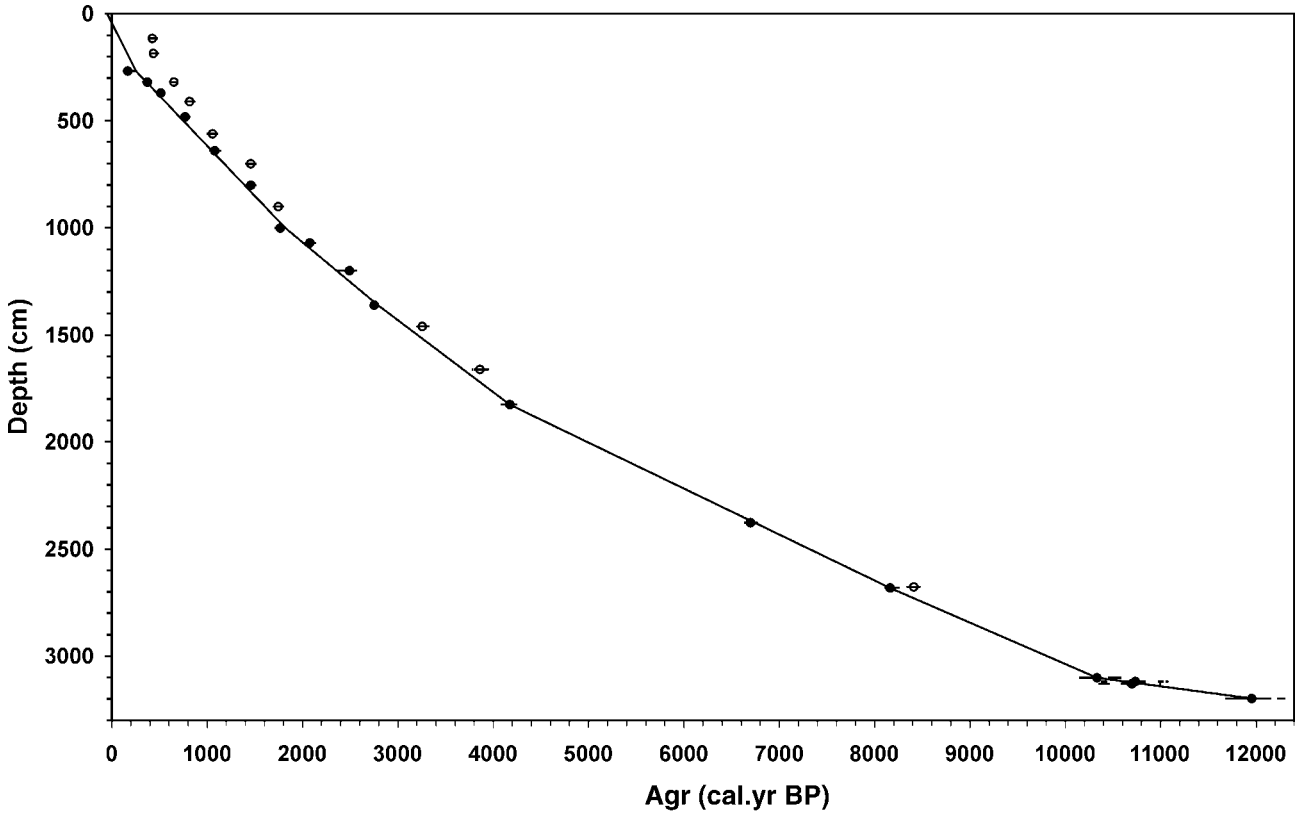

Figure 5 Age model for core MD99-2286 based on 27 AMS ^{14}C dates. The age model is shown with a line connecting filled circles. Open circles show age estimates excluded from the age model because of presumed sediment reworking. Error bars denote 1σ calibrated age ranges (see also Table 1)

in age to the closest underlying sample. This pattern cannot be explained by the order in which the samples were analysed since they were measured in random order (see laboratory codes in Table 1). Anomalously old ages could be explained by sub-depositional reworking or by contamination with older carbon, whereas anomalously young ages could be explained by contamination with modern carbon or by deep burrowing of the dated species. Contamination errors are generally only likely in the foraminiferal samples, as these are not etched during pretreatment. Errors from deep burrowing are less likely as all of the dated mollusc species are known not to burrow more than ca. 10 cm into the substratum (Anders Warén, Museum of Swedish Natural History, personal communication, 2002). By assuming that all samples yielding ages older than or identical to the closest underlying samples are reworked, it follows that these 10 samples should be excluded from the construction of the age model (Fig. 5, dates in parentheses in Table 1). The age model for core Sk000209-2 is based on seven ^{210}Pb dates and two ^{14}C dates. The ^{210}Pb measurements in the top 25 cm of core Sk000209-2 produced consistent results and show that the core top is of modern (zero) age (Senneset, 2002) (Table 1).

High-resolution chirp sonar profiling

The chirp sonar acoustic stratigraphy generally shows acoustically stratified sediments with several internal parallel reflectors overlying a substratum, which was poorly penetrated by the chirp signal. Four seismo-acoustic units have been defined, labelled A, B, C and D from the top down (Fig. 6). These units are separated by prominent reflectors numbered 1, 2, 3 and 4 from the top down (Fig. 6). The three upper units A, B and C blanket the underlying topography and are distinguished by relatively low acoustic impedance and continuous internal layering. The lowermost unit D closely drapes the subjacent topography and shows internal layering and relatively high acoustic impedance. In some of the profiles, distinct depressions ranging from about 50 to about 200 m in diameter can be seen within or close to areas showing acoustic turbidity. These depressions, 11 in total, are interpreted as pockmarks. Acoustic turbidity obscured the chirp profiles in about one-third of the area covered. Acoustic turbidity is caused by a high gas content and is often found in relation to areas with pockmarks in the Skagerrak (Hovland and Judd, 1988; Judd and Hovland, 1992).

Unit D

Unit D is the lowermost unit, characterised by high acoustic impedance and defined by a sharp upper boundary at reflector 3. Distinctive parallel internal reflectors in unit D are continuous throughout the investigated area, and the thickness of unit D is relatively uniform at about 15 ms, equivalent to ca. 23 m. However, the lower boundary of unit D, reflector 4, is not a sharp reflector in all profiles, as the acoustic signal is completely absorbed within or immediately below this unit. Unit D closely drapes the underlying surface, so that the topography of the substratum is more or less preserved throughout the sediment unit.

Unit C

Unit C is defined as the virtually acoustically transparent unit between the weak reflector 2 and the strong reflector 3. Unit

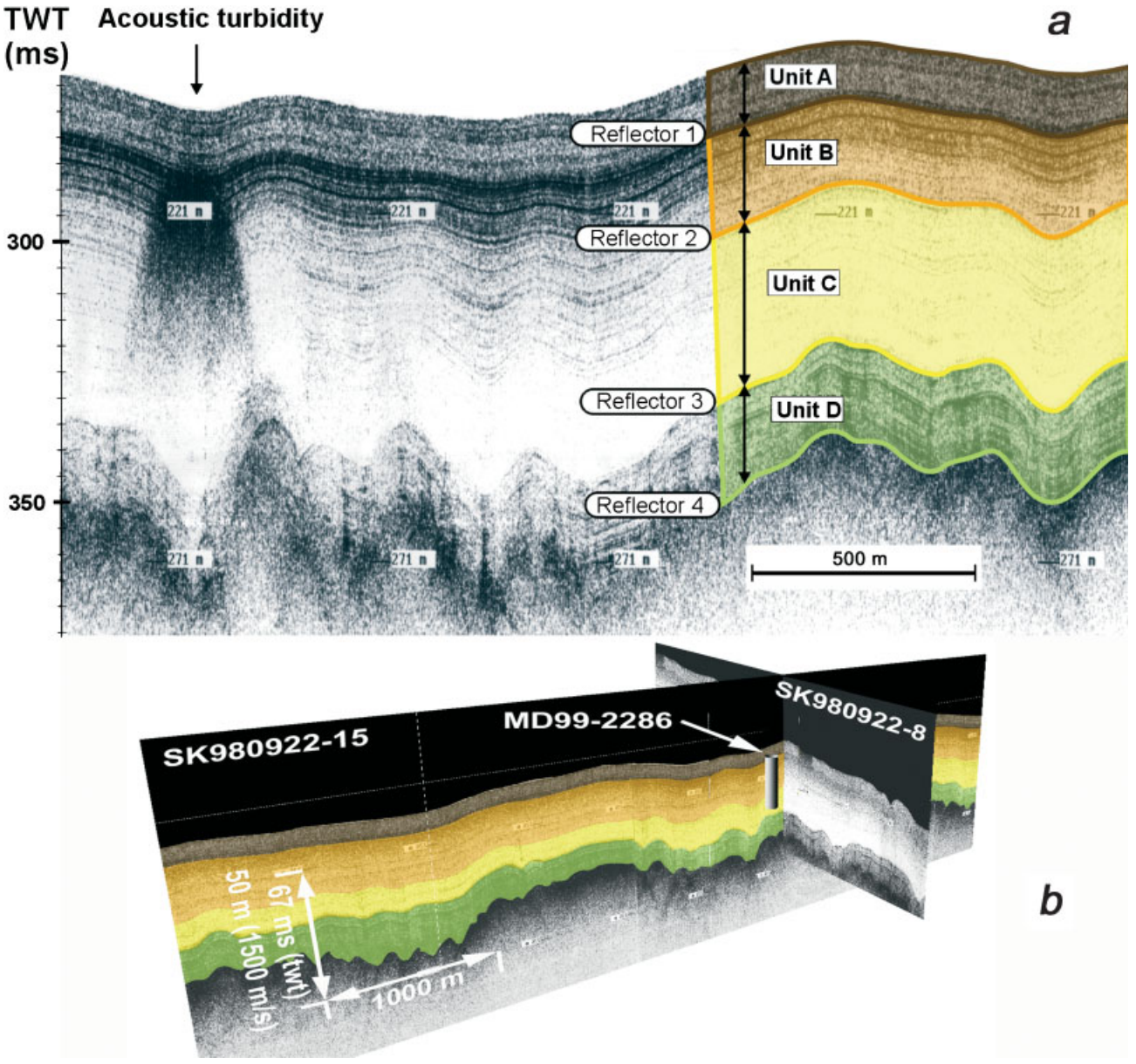

Figure 6 (a) Representative chirp record from a section located at N58°43.9′, E10°14.6′, showing the general stratigraphy of the survey area in northeastern Skagerrak. The defined seismic reflectors 1–4 and units A–D are indicated. A patch of acoustic turbidity is marked with an arrow. Depth labels in metres are based on 1500 m s^{-1} sound velocity. (b) Oblique 3-D view of the chirp sonar profiles around the coring location of MD99-2286 (see crossing white lines in Fig. 2). The chirp profile names are indicated, and core MD99-2286 is marked with a grey cylinder below the arrow. Colours on the chirp profiles mark interpreted seismic units

C has a varying thickness, ranging from about 20 to about 35 ms, equivalent to ca. 30–53 m. The acoustic impedance is generally relatively low in unit C, and decreases from reflector 2 downwards. Unit C is acoustically transparent to the chirp sonar pulse used in this survey in the lowermost part of the unit. Only a few, weak internal reflectors with low continuity are present in unit C.

Unit B

Unit B is defined as the unit between reflectors 1 and 2. The thickness of unit B varies conformably with unit C and ranges from about 10 to about 25 ms, equivalent to ca. 15–38 m. Unit B is characterised by distinct acoustic layering in the top and declining acoustic impedance downwards from reflector 1. Reflector 2 is weak in comparison to reflectors 1, 3 and 4 and has moderate to low continuity.

Unit A

Unit A is the uppermost unit, defined by an upper boundary at the seafloor and by a lower boundary at reflector 1. Unit A has a relatively uniform thickness of about 10–12 ms, equivalent to ca. 15–18 m, and is characterised by moderate acoustic impedance throughout the investigated area, and weak but clearly parallel layering. The acoustic impedance increases towards reflector 2. Many of the profiles show acoustic turbidity (Fig. 6), which in all but a few cases have an upper boundary within unit A.

Discussion

Core/seismic integration

In order to get a better understanding of what causes the observed seismo-acoustic reflectors, it is important to obtain

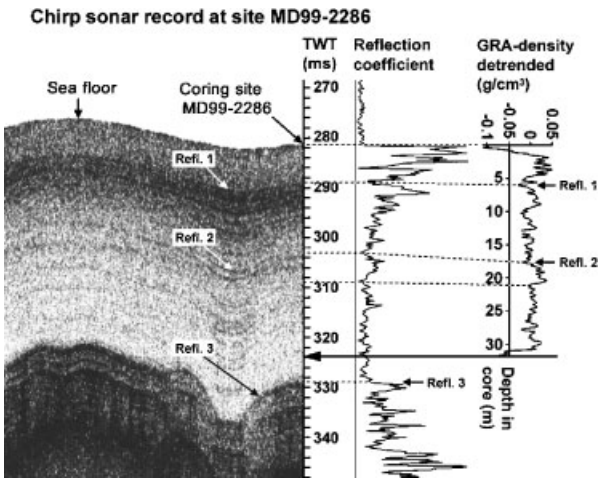

Figure 7 Proposed correlation of the MST-measured GRA-density log with the chirp sonar profile at the coring site. The reflection coefficient is shown as measured by the chirp sonar for the seismic trace at the coring location. The GRA-density log was linearly detrended in order to compensate for the effect of compaction, and was smoothed using a 27-term Gaussian filter. The length of the GRA-density log depth scale was adjusted to the sound velocity used by the chirp sonar ($1500\,m\,s^{-1}$), and the inferred penetration depth is indicated with an arrow. Reflector 1 and 2 (defined in Fig. 6) are marked by sharp density contrasts in the log

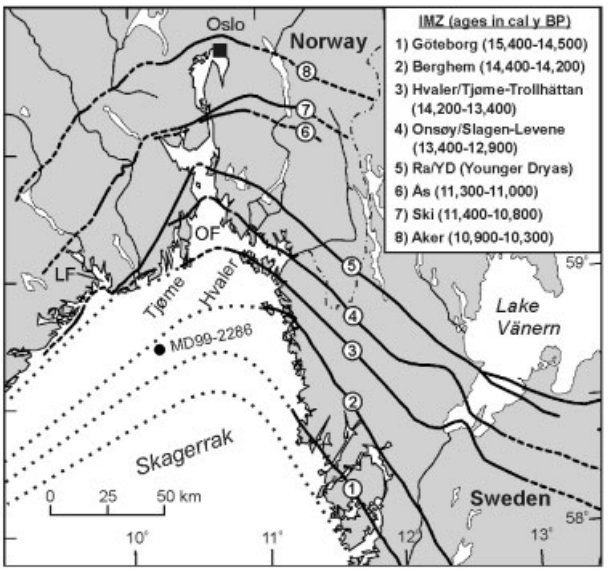

Figure 8 Ice Marginal Zones (IMZ, numbers in circles) of the Oslo Fjord region and southwestern Sweden, compiled from Andersen *et al.* (1995a), Sørensen (1992), and Lundqvist and Wohlfarth (2001). Solid lines indicate mapped IMZ positions, and dashed lines mark inferred ice margins. The dotted lines mark hypothetical offshore ice margins inferred from ice flow lineations (Kleman *et al.*, 1997; Boulton *et al.*, 2001). Ages for IMZ 1, 2, 4 and 5 and the oldest IMZ 3 age are from Lundqvist and Wohlfarth (2001). The youngest IMZ 3 age located at Tjøme (see text) and ages for IMZ 6–8 are calibrated in this work from ^{14}C ages of Andersen *et al.* (1995a). LF and OF marks the Langesundsfjord and the Oslo Fjord, respectively. The black dot shows the location of core MD99-2286

a reliable correlation between the core and the seismo-acoustic record at the coring site. Optimally, this is carried out using density and p-wave velocity data from the core to calculate the acoustic reflectivity function and generate a synthetic seismogram through convolution with the seismo-acoustic source function. The modelled acoustic trace may then be directly compared to the traces in the seismo-acoustic records from the coring site. The p-wave velocity measurements of core MD99-2286 are not of sufficient quality for this purpose due to poor transducer coupling (Fig. 4b). However, the GRA-density record shows changes that would give rise to pronounced acoustic impedance contrasts that probably caused reflections in the chirp pulse. Based on the GRA-density record a core-/seismo-acoustic correlation is proposed in Fig. 7.

Interpretation of chirp sonar profiles

Unit D

Based on the pronounced stratification and the draping appearance, Unit D is interpreted as glacial marine sediments ('inner proximal zone', Boulton, 1990), mainly formed from rapid deposition of suspended matter. The acoustic pattern with strong, closely spaced reflectors conformable with the underlying bedrock (Figs 6 and 8) is characteristic for ice-proximal glacial marine sediments consisting of beds of alternating sand/gravel and mud (Syvitski, 1991; Syvitski *et al.*, 1996). This facies association is produced by highly sediment-charged subglacial meltwater streams proximal to tidewater-glaciers (Powell, 1981). Unit D may be correlated to unit 2 of van Weering (1973; 1975; 1982a), Solheim and Grønlie (1983), and Holtedahl (1986), sequence 2 of Salge and Wong (1988), sequence P4 of von Haugwitz and Wong (1993), unit G of Rise *et al.* (1996) and unit C of Novak and Stoker (2001).

The lower boundary of unit D, reflector 4, is generally weak and in some profiles missing, as the acoustic signal is completely absorbed within or immediately below unit D (Figs 6 and 7). Unit D thus appears to be underlain by a dense, compacted substratum, such as till or diamicton, or rests directly on the bedrock surface. However, either proposed cases of substratum composition imply that reflector 4 marks the onset of glacial marine sedimentation in the area after the ground-based ice had retreated and started to float over the deeper basins. It follows that the age of reflector 4, i.e. the base of unit D, must be close to the timing of the ice-retreat from the area.

As the sea level rose during the deglaciation, a floating ice shelf, calving icebergs into a fully marine environment, developed in the deeper parts of the Skagerrak basin between ca. 17 000 and 15 000 cal. yr BP. When the ice shelf broke up, the ice margin rapidly receded to a grounding line in northeastern Skagerrak (southernmost dotted line in Fig. 8), reaching the present Swedish west coast at ca. 15 000 cal. yr BP (Andersen *et al.*, 1995b; Lagerlund and Houmark-Nielsen, 1993; Kleman *et al.*, 1997; Lundqvist and Wohlfarth, 2001; Houmark-Nielsen and Kjaer, 2003). Dated moraines onshore provide age estimates of the position of the ice margin when it had reached the present coast (Fig. 8). The ice marginal deposits on the Hvaler islands, eastern outer Oslo Fjord, are correlated to the east with the Trollhättan Moraine in Sweden (Berglund, 1979; Sørensen, 1979, 1992; Andersen *et al.*, 1995a), which formed ca. 14 100–14 200 cal. yr BP after a period of rapid ice-retreat (Lundqvist and Wohlfarth, 2001). The Hvaler moraines are correlated to the west with ice marginal deposits on Tjøme in the western outer Oslo Fjord (Sørensen, 1992; Andersen *et al.*, 1995a).

The recession was fastest in the northeastern to northern direction (Longva and Thorsnes, 1997; Boulton *et al.*, 2001). Based on the recession diagrams compiled by Andersen *et al.* (1995a), the ice recession rate on the eastern and western side of the outer Oslo Fjord was ca. 30–40 m yr^{-1} during the last deglaciation. However, the Berghem Moraine, located ca.

20 km towards the coast from the Trollhättan Moraine, was formed ca. 14 400–14 200 cal. yr BP (Lundqvist and Wohlfarth, 2001), which suggests an ice recession rate in this area well over 100 m yr^{-1} (Fig. 8). As marine parts of the ice sheet decayed faster than the land ice through iceberg calving (Lagerlund and Houmark-Nielsen, 1993; Longva and Thorsnes, 1997; Siegert *et al.*, 2001), an ice recession rate on the order of 100–200 m yr^{-1} appears reasonable. Tjøme is located ca. 40 km north-northeast of the MD99-2286 coring site, and is the closest locality where the deglaciation is dated. The Tjøme moraine was formed 11 975 ± 155 ^{14}C years BP, which was calibrated to a median age of 13 420 cal. yr BP (one-sigma range 13 170–13 670 cal. yr BP) using the same calibration parameters as for the core MD99-2286 dates (this work), and gives a minimum age for the Hvaler/Tjøme–Trollhättan IMZ (Andersen *et al.*, 1995a). To conclude, the bounding parameters for estimation of the deglaciation age of the coring site are the end member ages of the Tjøme (ca. 13 200–13 600 cal. yr BP) and Trollhättan (14 100–14 200 cal. yr BP) moraines and an assumed ice recession rate of 100–200 m yr^{-1} over a distance of 40 km. From this, it follows that the coring site was presumably deglaciated between 14 600 (14 200 ± 400) and 13 400 (13 200 ± 200) cal. yr BP, which thus constitutes a maximum age for unit D sediments.

The total sediment thickness below core MD99-2286 amounts to about 25 ms (ca. 19 m) (Figs 6b and 7). In principle, we lack age control from the base of the core to the base of unit D, preventing firm conclusions about sedimentation rates from this interval. Yet, some reasonable speculations can be made about the sedimentation rate in this interval. The time available for deposition of unit D and lowermost unit C is on the order of 2000 years, counted from the possible onset of sedimentation after the deglaciation at 14 600–13 400 cal. yr BP to the base of core MD99-2286 at ca. 12 000 cal. yr BP. This implies an average sedimentation rate on the order of 1 cm yr^{-1} for the deposition of this sedimentary succession. However, unit D is interpreted to consist of ice-proximal sediments, and sedimentation rates in the proximal zone (ca. < 40 km, Boulton, 1990) of a melting and calving ice sheet decrease exponentially from the glacier front. When the ice is retreating, sediment accumulation is largely controlled by the rate of retreat (Eyles *et al.*, 1985; Syvitski, 1989; Boulton, 1990). This implies that the sedimentation rate was initially very high during deposition of unit D, but then decreased significantly with time. Given ice recession rates of 100–200 m yr^{-1}, the time of rapid (ice proximal) deposition of unit D is restricted to ca. 200–400 years after deglaciation, before the investigated area was in a distal (ca. > 40 km, Boulton, 1990) position to the ice front and sedimentation rates were significantly lowered. This interpretation is coherent with results from the Troll 3.1 core and adjacent seismic profiles, which indicate that deposition of ice-proximal sediments lasted only a few hundred years (Andersen *et al.*, 1995b). It is also consistent with the results from Solheim and Grønlie (1983), who proposed that their unit 2 in the outer Oslo Fjord was rapidly deposited under ice-proximal conditions, although a maximum of 3000 years for deposition of this unit was suggested.

Deposition of unit D was probably initiated when the ice retreated far enough to permit adjacent fjords to act as sediment traps. Thick sequences of glacial marine sediments have been reported from seismic studies of the Oslo Fjord (Solheim and Grønlie, 1983; Pederstad *et al.*, 1993) and the Langesundsfjord (Holtedahl, 1986) and their associated submarine channels. Some of the deepest parts of the Oslo Fjord were ice-free by ca. 13 400 cal. yr BP (see Levene moraine, Fig. 8). We propose that the sharp boundary between Unit C and D, reflector 3 (Figs 6 and 7), represents the break-up of the ice shelf and rapid recession of the ice front to a more distal position. Accordingly, reflector 3 is proposed to have formed mainly as a result of a drastic lowering of the sedimentation rate, for which sediments being trapped in newly deglaciated fjord and channel systems in southeastern Norway probably had a major effect. A similar development was proposed for the formation of the upper boundary reflector of unit F of Andersen *et al.* (1995b) based on seismic profiles adjacent to the Troll 3.1 core. After formation of reflector 3, distal glacial marine processes gained dominance over ice-proximal glacial marine sedimentation. This is consistent with the results from Salge and Wong (1988), who proposed that the sedimentation rate in the Skagerrak was about ten times higher in the Late Pleistocene than in the Holocene. It is also consistent with the results from the Troll 3.1 core by Andersen *et al.* (1995b), who concluded that the sedimentation rate in the Norwegian Channel was rapidly lowered by several orders of magnitude at the beginning of the Younger Dryas at 11 300 ^{14}C years BP (ca. 12 900 cal. yr BP, this work).

Unit C

The weak, but continuous parallel reflectors blanketing the subjacent topography indicate very fine-grained nearly homogeneous material, deposited under calm conditions (Figs 6 and 7). Unit C is interpreted as distal glacial marine sediments gradually changing to postglacial marine sediments deposited during latest Pleistocene to early Holocene times. This is consistent with the interpretation of the uppermost unit H of von Haugwitz and Wong (1993). They concluded that by the end of the Pleistocene, shallow marine deposits gradually came to dominate over glacial marine sediments. As the sea level rose, the main depocentre for the postglacial marine sediments shifted to the east, causing the sedimentation rate in the eastern Skagerrak to increase throughout the early Holocene.

The unit C sediments below core MD99-2286 amounts to ca. 10 ms (ca. 8 m) (Figs 6b and 7), and the linear sedimentation rate in the bottom of core MD99-2286 is ca. 0.06 cm yr^{-1}. Considering the time available for deposition of this succession, maximum ca. 2000 years (as discussed above), the average sedimentation rate must have been significantly higher during deposition of lowermost unit C than in the parts recovered in core MD99-2286. An explanation for this could be that the shoreline displacement resulting from the rapid isostatic uplift commencing immediately after deglaciation (Hafsten, 1983; Lambeck *et al.*, 1998) probably exposed substantial amounts of material to erosion and transport into the Skagerrak. Such a development was previously suggested for deposition of the lowermost part of the upper, previously supposed Holocene unit of Solheim and Grønlie (1983), Holtedahl (1986) and Rise *et al.* (1996).

Reflector 3 is the most prominent reflector in the chirp sonar profiles (Figs 6 and 7). This reflector has a wide regional extent, and its strong reflection coefficient and good continuity permits correlation with previous investigations (van Weering *et al.*, 1973; van Weering, 1975, 1982b; Fält, 1982; Holtedahl, 1986; Salge and Wong, 1988; von Haugwitz and Wong, 1993; Andersen *et al.*, 1995b; Rise *et al.*, 1996). In these studies, the correlated reflector is interpreted to represent the Pleistocene/Holocene boundary, which is dated to 11 500 cal. yr BP according to the informal working definition of the International Commission on Stratigraphy (ICS website, 2004). Reflector 3 may be correlated to reflector U_5 of von Haugwitz and Wong (1993). They conclude that reflector U_5 represents an unconformity. Although reflector 3 of the present survey is very sharp, the chirp sonar profiles do not indicate any

truncated reflectors or the presence of an unconformity. Using the age model for core MD99-2286 and an estimate of the core penetration in the chirp sonar profiles, the validity of the previous assumption of a Pleistocene/Holocene boundary age for reflector 3 can be assessed.

The bottom of core MD99-2286 at 32 m is AMS ^{14}C dated to 10 715 ± 80 ^{14}C years, corresponding to 11 950 (+350/−275) cal. yr BP. The corresponding penetration depth of core MD99-2286 in the chirp sonar profile at the coring site is 43 ms, assuming a sound velocity in the sediment of 1500 m s^{-1}. Accordingly, the total sediment thickness of unit A, B and C is 53 ms, implying that the core is 10 ms short of reaching reflector 3 (top of unit D). This suggested penetration depth is supported by the proposed correlation of core MD99-2286 with the chirp sonar profile based on GRA-density (Fig. 7). There is no apparent sharp boundary in the chirp sonar profiles at the depth of the Pleistocene/Holocene transition (11 500 cal. yr BP) inferred from the MD99-2286 age model. In order to obtain a core penetration that reaches reflector 3, one must assume a p-wave velocity of around 1200 m s^{-1}, which is unreasonable as the measured p-wave velocity in core MD99-2286 shows consistent values in the range of 1450 to 1550 m s^{-1}. Therefore, we propose that the sharp boundary between unit C and unit D, reflector 3, does not represent the base of the Holocene, as interpreted in earlier investigations (van Weering *et al.*, 1973; van Weering, 1975, 1982b; Solheim and Grønlie, 1983; Holtedahl, 1986; Salge and Wong, 1988; von Haugwitz and Wong, 1993; Rise *et al.*, 1996; Novak and Stoker, 2001).

Units B and A

The units above unit C represent postglacial marine sediments deposited from suspension under calm conditions, based on the relatively transparent but conformably stratified layers blanketing the underlying topography (Figs 6 and 7). Since the opening of the English Channel at ca. 8500 cal. yr BP, the Jutland Current has been one of the most important sources of sediment input to the eastern Skagerrak. The present-day Jutland Current (Fig. 3) is highly unstable and can be periodically blocked by inflowing Atlantic water, with subsequent flushing of sediment-loaded water into the deposition areas (Aure *et al.*, 1990). Bottom current pulses related to Jutland Current fluctuations during the last 2000 years were interpreted from grain size data in four cores from the southern flank of the Skagerrak (Hass, 1996). These current pulses were associated with colder periods with intensified storminess and increased westerly winds, but it is not known when this current behaviour started. However, the major components of the modern circulation system were established in conjunction with a hydrographic shift at ca. 6400 cal. yr BP manifested by an intensified flow of the Jutland Current (Conradsen, 1995; Conradsen and Heier-Nielsen, 1995; Jiang *et al.*, 1997). It is thus possible that the pulsating nature of the Jutland Current has been present since about mid-Holocene times. If this is correct, the relatively strong reflector 1, separating units A and B, as well as the internal reflectors within units A and B, could represent event-layers from periods of blocking and subsequent flushing of the Jutland Current. This would result in decreased current speed and consequent deposition of finer sediments followed by a sudden increase in current speed and deposition of more coarse-grained material, possibly causing reflectors in seismic profiles. This relationship needs to be further investigated by, for example, detailed grain-size analysis of core MD99-2286. The increasing sedimentation rate from upper unit C until recent, as measured in core MD99-2286, is probably a result of increasing sediment supply via the Jutland Current.

Conclusions

Based on high-resolution chirp sonar profiling and physical properties of a 32 m long piston core, the stratigraphy of uppermost Pleistocene to Holocene sediments in the northeastern Skagerrak has been described. Core MD99-2286 represents an apparently undisturbed high-resolution record of the entire Holocene and latest Pleistocene sediments, based on a radiocarbon-based age model and physical properties data.

The chirp sonar stratigraphy shows acoustically stratified sediments with several internal parallel reflectors overlying a rough-surfaced substratum not penetrated by the signal. The lowermost unit, D, is interpreted as ice-proximal glacial marine sediments rapidly deposited below or close to a calving shelf ice, until the ice shelf broke up and the ice front receded to a more distal position. The sharp boundary between Units C and D, reflector 3, is proposed to represent the rapid break-up of the ice-shelf and recession of the ice front far enough to expose the nearby fjords as sediment traps, causing a rapid lowering of the sedimentation rate in the investigated area. After this, postglacial marine processes gradually became dominant over glacial marine sedimentation.

Based on the suggested correlation of the ^{14}C dated core MD99-2286 with the chirp sonar profile, the prominent reflector separating the topmost relatively transparent unit from the underlying stratified unit is proposed to be older than the Pleistocene/Holocene boundary, as assumed in previous investigations. Instead, the change to Holocene conditions in the survey area in northeastern Skagerrak is interpreted to have occurred as a continuous process of increasingly normal marine deposition, which gradually substituted the distal glacial marine sedimentation. The base of the Holocene at 11 500 cal. yr BP is not represented by any seismically significant impedance contrasts. During deposition of the lowermost part of unit C, the average sedimentation rates must have been significantly higher than the rate measured in the bottom of core MD99-2286 at ca. 12 000 cal. yr BP, based on the correlation between the core and the chirp sonar profiles. Such high sedimentation rates could be caused by current reworking of near-coastal sediments that were exposed as the sea level was rapidly lowered due to glacio-isostatic rebound.

The uppermost units, B and A, represent marine Holocene sediments deposited with an increasing sedimentation rate reflecting a strengthening of the Jutland Current in an otherwise more or less modern oceanographic environment.

Acknowledgements We are grateful to Eve Arnold, Fredrik Klingberg and Tom Flodén for many fruitful discussions; Karen Luise Knudsen, Thomas Andrén and Jan Heinemeier for age model discussions; Jan Lundqvist for discussions on ice recession; Peter Kristensen for picking forams for radiocarbon dating; Liv Senneset for data from core Sk000209-2; the Geological Survey of Norway for generously provided bathymetric data; and two anonymous reviewers for constructive criticism.

References

Andersen BG, Mangerud J, Sørensen R, Reite A, Sveian H, Thoresen M, Bergström B. 1995a. Younger dryas ice-marginal deposits in Norway. *Quaternary International* **28**: 147–169.

Andersen ES, Østmo SR, Forsberg CF, Lehman SJ. 1995b. Late- and post-glacial depositional environments in the Norwegian Trench, northern North Sea. *Boreas* **24**: 47–64.

Andrén T, Lindeberg G, Andrén E. 2002. Evidence of the final drainage of the Baltic Ice Lake and the brackish phase of the Yoldia Sea in glacial varves from the Baltic Sea. *Boreas* **31**: 226–238.

Aure J, Svendsen E, Rey F, Skjoldal HR. 1990. The Jutland Current: nutrients and physical oceanographic conditions in late autumn 1989. *ICES Journal of Marine Science* **35**: 28 pp.

Bard E, Hamelin B, Fairbanks RG, Zindler A. 1990. Calibration of the ^{14}C timescale over the past 30 000 years using mass spectrometric U–Th ages from Barbados corals. *Nature* **345**: 405–410.

Berglund BE. 1979. The deglaciation of southern Sweden 13 500–10 000 B.P. *Boreas* **8**: 89–118.

Björck S. 1995. A review of the history of the Baltic Sea, 13.0–8.0 ka BP. *Quaternary International* **27**: 19–40.

Björck J, Andrén T, Wastegård S, Possnert G, Schoning K. 2002. An event stratigraphy for the Last Glacial–Holocene transition in eastern middle Sweden: results from investigations of varved clay and terrestrial sequences. *Quaternary Science Reviews* **21**: 1489–1501.

Bøe R, Rise L, Thorsnes T, de Haas H, Saether OM, Kunzendorf H. 1996. Sea-bed sediments and sediment accumulation rates in the Norwegian part of Skagerrak. *Norges Geologiske Undersøkelse* **430**: 75–84.

Bondevik S, Birks HH, Gulliksen S, Mangerud J. 1999. Late Weichselian marine ^{14}C reservoir ages at the western coast of Norway. *Quaternary Research* **52**: 104–114.

Boulton GS. 1990. Sedimentary and sea level changes during glacial cycles and their control on glacimarine facies architecture. In *Glacimarine Environments: Processes and Sediments*, vol. 53, Dowdeswell JA, Scourse JD (eds). Geological Society Special Publication no. 53; 15–52.

Boulton GS, Dongelmans P, Punkari M, Broadgate M. 2001. Palaeoglaciology of an ice sheet through a glacial cycle: the European ice sheet through the Weichselian. *Quaternary Science Reviews* **20**: 591–625.

Boyce RE. 1976. Definitions and laboratory techniques of compressional sound velocity parameters and wet-water content, wet-bulk density, and porosity parameters by gravimetric and gamma-ray attenuation techniques. In *Initial Reports of the Deep Sea Drilling Program 33*, vol. 33, Schlanger SO, Jackson ED, *et al*. (eds). U.S. Govt. Printing Office: Washington, DC; 931–958.

Conradsen K. 1995. Late Younger Dryas to Holocene palaeoenvironments of the southern Kattegat, Scandinavia. *The Holocene* **5**: 447–456.

Conradsen K, Heier-Nielsen S. 1995. Holocene paleoceanography and paleoenvironments of the Skagerrak–Kattegat, Scandinavia. *Paleoceanography* **10**: 801–813.

Eisma D, Kalf J. 1987. Dispersal, concentration and deposition of suspended matter in the North Sea. *Journal of the Geological Society of London* **144**: 161–178.

Eyles CH, Eyles N, Miall AD. 1985. Models of glacimarine sedimentation and their application to the interpretation of ancient glacial sequences. *Palaeogeography, Palaeoclimatology, Palaeoecology* **51**: 15–84.

Fält L-M. 1982. *Late Quaternary sea-floor deposits off the Swedish west coast*. PhD thesis, Chalmers University of Technology and University of Gothenburg. Publ A 37 (Göteborg).

Flodén T. 1973. Notes on the bedrock of the eastern Skagerrak with remarks on the pleistocene deposits. *Stockholm Contributions in Geology* **XXIV:5**: 79–102.

Hafsten U. 1983. Shore-level changes in south Norway during the last 13 000 years, traced by biostratigraphical methods and radiometric datings. *Norsk Geografisk Tidsskrift* **37**: 63–79.

Hajdas I, Beer J, Bonani G, Bonino G, Cini Castagnoli G, Taricco C. 1997. Radiocarbon time scale of the Mediterranean core CT85-5: the last 40 000 years. In *Proceedings of the International School of Physics 'Enrico Fermi' Course CXXXIII*, Cini Castagnoli G, Provenzale A (eds). IOS Press: Amsterdam.

Hass HC. 1996. Northern Europe climate variations during late Holocene: evidence from marine Skagerrak. *Palaeogeography, Palaeoclimatology, Palaeoecology* **123**: 121–145.

Holtedahl H. 1986. Sea-floor morphology and Late Quaternary sediments south of the Langesundsfjord, north-eastern Skagerrak. *Norsk Geologisk Tidsskrift* **66**: 311–323.

Houmark-Nielsen M, Kjaer KH. 2003. Southwest Scandinavia, 40–15 kyr BP: paleogeography and environmental change. *Journal of Quaternary Science* **18**: 769–786.

Hovland M, Judd AG. 1988. *Seabed Pockmarks and Seepages—Impact on Geology, Biology and the Marine Environment*. Graham & Trotman: London; 180–203.

ICS website. 2004. Overview of Global Boundary Stratotype Sections and Points (GSSPs). http://www.stratigraphy.org [20 July 2004].

IOC, IHO, BODC. 2003. Centenary Edition of the General Bathymetric Chart of the Oceans (GEBCO) Digital Atlas (GDA). Intergovernmental Oceanographic Commission and the International Hydrographic Organization as part of the General Bathymetric Chart of the Oceans, British Oceanographic Data Centre, Liverpool.

Jelgersma S. 1979. Sea-level changes in the North Sea basin. In *The Quaternary History of the North Sea*, Oerle E, Shüttenhelm RTE, Wiggers AJ (eds). Acta Univ. Ups. Symp. Univ. Ups. Annum Quingentesimum Celebrantis, 2: Uppsala; 233–248.

Jiang H, Björck S, Knudsen KL. 1997. A palaeoclimatic and palaeoceanographic record of the last 11 000 ^{14}C years from the Skagerrak–Kattegat, north-eastern Atlantic margin. *The Holocene* **7**: 301–310.

Judd AG, Hovland M. 1992. The evidence of shallow gas in marine sediments. *Continental Shelf Research* **12**: 1081–1095.

Kleman J, Hättestrand C, Borgström I, Stroeven A. 1997. Fennoscandian paleoglaciology reconstructed using a glacial geological inversion model. *Journal of Glaciology* **43**: 283–299.

Knudsen KL, Seidenkrantz M-S. 1998. Holocene palaeoenvironments in the North Sea region: reflections from the Skagen core. In *Geoscience in Aarhus Presented in Connection with the 23rd Nordic Geological Winter Meeting*, Wilson JR, Michelsen Ø (eds). Aarhus, Denmark; 45–48.

Lagerlund E, Houmark-Nielsen M. 1993. Timing and pattern of the last deglaciation in the Kattegat region, southwest Scandinavia. *Boreas* **22**: 337–347.

Lambeck K. 1995. Late Devensian and Holocene shorelines of the British Isles and North Sea from models of glacio-hydro-isostatic rebound. *Journal of the Geological Society of London* **152**: 437–448.

Lambeck K, Smither C, Johnston P. 1998. Sea-level change, glacial rebound and mantle viscosity for northern Europe. *Geophysical Journal International* **134**: 102–144.

Leth JO. 1996. Late Quaternary geological development of the Jutland Bank and the initiation of the Jutland Current, NE North Sea. *Geological Survey of Norway Bulletin* **430**: 25–34.

Longva O, Thorsnes T. 1997. Skagerrak in the past and present—an integrated study of geology, chemistry, hydrography and microfossil ecology. In *NGU Special Publication*, no. 8; 1–100.

Lundqvist J, Wohlfarth B. 2001. Timing and east–west correlation of south Swedish ice marginal lines during the Late Weichselian. *Quaternary Science Reviews* **20**: 1127–1148.

Mayer LA, Paton CW, Gee L, Gardner JV, Ware CW. 2000. Interactive 3-D visualization: a tool for seafloor navigation, exploration, and engineering. *Proceedings of IEEE Oceans* **2**: 913–920.

Nordberg K. 1991. Oceanography in the Kattegat and Skagerrak over the past 8000 years. *Paleoceanography* **6**: 461–484.

Novak B, Stoker MS. 2001. Late Weichselian glacimarine depositional processes in the southern Skagerrak revealed by high-resolution seismic facies analysis. *Marine Geology* **178**: 115–133.

Ottesen D, Bøe R, Longva O, Olsen HA, Rise L, Skilbrei JR, Thorsnes T. 1997. Geologisk atlas—Skagerrak. Atlas over kvartaere avsetninger, bunnsedimenter, berggrunn og batymetri i norsk sektor av Skagerrak. *NGU Rapport* no. 96; 138 pp.

Otto L, Zimmerman TF, Furnes GK, Mork M, Saetre R, Becker G. 1990. Review of the physical oceanography of the North Sea. *Netherlands Journal of Sea Research* **26**: 161–238.

Pederstad K, Roaldset E, Roenningsland TM. 1993. Sedimentation and environmental conditions in the inner Skagerrak–outer Oslofjord. *Marine Geology* **111**: 245–268.

Powell RD. 1981. A model for sedimentation by tidewater glaciers. *Annals of Glaciology* **2**: 129–134.

Rack F, Skinner A, Amman H. 2000. Coring and high pressure sampling. In *Proceedings from INMARTECH 2000 International Marine*

Technicians Workshop 20–22 September, Robertson KG, Rietveld MJ (eds). Royal Netherlands Institute for Sea Research (NIOZ), Texel; 113–119.

Rise L, Olsen HA, Bøe R, Ottesen D. 1996. Thickness, distribution and depositional environment of Holocene sediments in the Norwegian part of Skagerrak. *Norges geologiske Undersøkelse* **430**: 5–16.

Rodhe J. 1987. The large-scale circulation in the Skagerrak: interpretation of some observations. *Tellus* **39A**: 245–253.

Rodhe J. 1998. The Baltic and North Seas: a process-oriented review of the physical oceanography. In *The Sea*, vol. 11, Robinson AR, Brink KH (eds). Wiley: New York; 699–732.

Rodhe J, Holt N. 1996. Observations of the transport of suspended matter into the Skagerrak along the western and northern coast of Jutland. *Journal of Sea Research* **35**: 91–98.

Salge U, Wong HK. 1988. Seismic stratigraphy and Quaternary sedimentation in the Skagerrak (north-eastern North Sea). *Marine Geology* **81**: 159–174.

Schock SG, LeBlanc LR, Mayer LA. 1989. Chirp subbottom profiler for quantitative sediment analysis. *Geophysics* **54**: 445–450.

Sejrup HP, Aarseth I, Haflidason H, Løvlie R, Bratten Å, Tjøstheim G, Forsberg CF, Ellingsen KL. 1995. Quaternary of the Norwegian Channel: glaciation history and palaeoceanography. *Norsk Geologisk Tidsskrift* **75**: 65–87.

Sejrup HP, Larsen E, Landvik J, King EL, Haflidason H, Nesje A. 2000. Quaternary glaciations in southern Fennoscandia: evidence from southwestern Norway and the northern North Sea region. *Quaternary Science Reviews* **19**: 667–685.

Sejrup HP, Larsen E, Haflidason H, Berstad IM, Hjelstuen BO, Jonsdottir HE, King EL, Landvik J, Longva O, Nygard A, Ottesen D, Raunholm S, Rise L, Stalsberg K. 2003. Configuration history and impact of the Norwegian Channel Ice Stream. *Boreas* **32**: 18–36.

Senneset L. 2002. *A record of high resolution ocean variability from Skagerrak over the past 900 years*. Masters thesis, University of Bergen (Bergen).

Siegert MJ, Dowdeswell JA, Hald M, Svendsen J-I. 2001. Modelling the Eurasian Ice Sheet through a full Weichselian glacial cycle. *Global and Planetary Change* **31**: 367–385.

Solheim A, Grønlie G. 1983. Quaternary sediments and bedrock geology in the outer Oslofjord and northernmost Skagerrak. *Norsk Geologisk Tidskrift* **63**: 55–72.

Sørensen R. 1979. Late Weichselian deglaciation in the Oslofjord area, south Norway. *Boreas* **8**: 241–246.

Sørensen R. 1992. The physical environment of Late Weichselian deglaciation of the Olsofjord region, south-eastern Norway. *Sveriges Geologiska Undersökning Serie Ca* **81**: 339–346.

Stabell B, Thiede J. 1985. The physiographic evolution of the Skagerrak during the past 15 000 years: paleobathymetry and paleoceanography. *Norsk Geologisk Tidsskrift* **65**: 19–22.

Stabell B, Thiede J. 1986. Paleobathymetry and paleogeography of southern Scandinavia in the late Quaternary. *Meyniana* **38**: 43–59.

Stabell B, Werner F, Thiede J. 1985. Late Quaternary and modern sediments of the Skagerrak and their depositional environment: An Introduction. *Norsk Geologisk Tidsskrift* **65**: 9–17.

Stuiver M, Reimer PJ. 1993. Extended 14C data base and revised CALIB 3.0 ^{14}C age calibration program. *Radiocarbon* **35**: 215–230.

Stuiver M, Reimer PJ, Braziunas TF. 1998. High-precision radiocarbon age calibration for terrestrial and marine samples. *Radiocarbon* **40**: 1127–1151.

Svansson A. 1975. Physical and chemical oceanography of the Skagerrak and Kattegat. I. Open sea conditions. *Fishery Board of Sweden, Institute of Marine Research, Report*, no. 1; 88 pp.

Syvitski JPM. 1989. On the deposition of sediment within glacier-influenced fjords: oceanographic controls. *Marine Geology* **85**: 301–329.

Syvitski JPM. 1991. Towards an understanding of sediment deposition on glaciated continental shelves. *Continental Shelf Research* **11**: 897–937.

Syvitski JPM, Lewis CFM, Piper DJW. 1996. Palaeoceanographic information derived from acoustic surveys of glaciated continental margins: examples from eastern Canada. In *Late Quaternary Palaeoceanography of the North Atlantic Margins*, Andrews JT, Austin WEN, Bergsten H, Jennings AE (eds). Geological Society Special Publication no. 111; 51–76.

Telford RJ, Heegard E, Birks HJB. 2004. The intercept is a poor estimate of a calibrated radiocarbon age. *The Holocene* **14**: 296–298.

van Weering TCE. 1975. Late Quaternary history of the Skagerrak: an interpretation of acoustical profiles. *Geologie en Mijnbouw* **54**: 130–145.

van Weering TCE. 1982a. Recent sediments and sediment transport in the northern North Sea: pistoncores from Skagerrak. *Proceedings of the Koninklijke Nederlandse Akademie van Wetenschapper* **B85**: 155–201.

van Weering TCE. 1982b. Shallow seismic and acoustic reflection profiles from the Skagerrak: implications for recent sedimentation. *Proceedings of the Koninklijke Nederlandse Akademie van Wetenschapper* **B85**: 129–154.

van Weering TCE, Jansen JHF, Eisma D. 1973. Acoustic reflection profiles of the Norwegian Channel between Oslo and Bergen. *Netherlands Journal of Sea Research* **6**: 241–263.

van Weering TCE, Berger GW, Okkels E. 1993. Sediment transport, resuspension and accumulation rates in the north-eastern Skagerrak. *Marine Geology* **111**: 269–285.

von Haugwitz WR, Wong HK. 1993. Multiple Pleistocene ice advances into the Skagerrak: a detailed seismic stratigraphy from high resolution seismic profiles. *Marine Geology* **111**: 189–207.